Coordination of Interdependent Natural Gas and Electricity Infrastructures for Firming the Variability of Wind Energy in Stochastic Day-Ahead Scheduling

Ahmed Alabdulwahab, Abdullah Abusorrah, Xiaping Zhang, and Mohammad Shahidehpour, *Fellow, IEEE*

***Abstract*—In this paper, the coordination of constrained electricity and natural gas infrastructures is considered for firming the variability of wind energy in electric power systems. The stochastic security-constrained unit commitment is applied for minimizing the expected operation cost in the day-ahead scheduling of power grid. The low cost and sustainable wind energy could substitute natural gas-fired units, which are constrained by fuel availability and emission. Also, the flexibility and quick ramping capability of natural gas units could firm the variability of wind energy. The electricity and natural gas network constraints are considered in the proposed model (referred to as EGTran) and Benders decomposition is adopted to check the natural gas network feasibility. The autoregressive moving average (ARMA) time-series model is used to simulate wind speed forecast errors in multiple Monte Carlo scenarios. Illustrative examples demonstrate the effectiveness of EGTran for firming the variable wind energy by coordinating the constrained electricity and natural gas delivery systems.**

***Index Terms*—Day-ahead scheduling, natural gas, renewable energy, stochastic security-constrained unit commitment.**

NOMENCLATURE

Index:

s	Index of scenarios.
i	Index of generating units.
sp	Index of natural gas suppliers.
l	Index of natural gas loads.
br	Index of power transmission branches.
b	Index of buses.
t	Index of hours.
m, n	Index of nodes in natural gas network.
j, k	Index of buses in electric network.

Manuscript received August 17, 2014; revised November 05, 2014 and January 09, 2015; accepted January 15, 2015. Date of publication March 13, 2015; date of current version March 18, 2015. This work was supported by the Deanship of Scientific Research (DSR), King Abdulaziz University, Jeddah, Saudi Arabia under Grant Gr/34/6. Paper no. TSTE-00406-2014.

A. Alabdulwahab and A. Abusorrah are with the Renewable Energy Research Group, King Abdulaziz University, Jeddah, Saudi Arabia (e-mail: aabdulwhab@kau.edu.sa).

X. Zhang is with the Galvin Center for Electricity Innovation, Illinois Institute of Technology, Chicago, IL 60616, USA (e-mail: xzhan126@hawk.iit.edu).

M. Shahidehpour is with the Galvin Center for Electricity Innovation, Illinois Institute of Technology, Chicago, IL 60616, USA, and also with the Renewable Energy Research Group, King Abdulaziz University, Jeddah, Saudi Arabia.

Color versions of one or more of the figures in this paper are available online at http://ieeexplore.ieee.org.

Digital Object Identifier 10.1109/TSTE.2015.2399855

Variables:

I_i	Status indicator of generating unit i.
P_i	Generation dispatch of a unit i.
P_w	Generation dispatch of wind unit w.
DL_b	Loss of load at bus b at time t.
SR_i	Spinning reserve of a unit i.
$\mathrm{SU}_i, \mathrm{SD}_i$	Startup/shutdown cost of a unit i.
X_i^{on}	ON time of unit i, in hour.
X_i^{off}	OFF time of unit i, in hour.
F_i^c	Cost function of generating unit i.
F_i^e	Emission function of unit i.
$F_{\mathrm{i}}^{\mathrm{gas}}$	Fuel function of natural gas-fired unit i.
W_i^{gas}	Fuel cost of natural gas-fired unit i.
v_{sp}	Gas delivery amount of supplier sp.
L_l	Gas load of load l.
ω	Pressure of node.
f_{mn}	Natural gas flow from node m to n.
$\mathrm{pf}_{\mathrm{br}}$	Power flow through branch br.
θ	Bus voltage angle.

Constants:

Pr_s	Probability of scenario s.
N_S	Number of scenarios.
N_B	Number of load buses.
N_T	Number of time periods.
N_U	Number of generating units.
N_W	Number of wind power units.
$\mathrm{pf}_{\mathrm{br}}^{\max}$	Power flow limits of branch br.
EG	Set of units within same emission group.
$P_i^{\min}, P_i^{\max}$	Minimum and maximum capacity of unit i.
$R_i^{\mathrm{up}}, R_i^{\mathrm{dn}}$	Up/down limits for corrective dispatch of unit i.
$T_i^{\mathrm{on}}, T_i^{\mathrm{off}}$	Minimum ON/OFF time of unit i.
a_i^e, b_i^e, c_i^e	Coefficient of emission function of unit i.
$\mathrm{SU}_i^e, \mathrm{SD}_i^e$	Startup/shutdown emission of unit i.
$\mathrm{EMS}^{\max}$	Regional/system emission upper limit.
PW_w^f	Generation forecast for wind unit w.
DE_b	Load forecast at bus b.
$\mathrm{DL}_b^{\max}$	Maximum load shedding level at bus b.
VOLL	Value of lost load ($/MW/h).
R	System spinning reserve.
NGS	Number of natural gas suppliers.
NGL	Number of natural gas loads.
GU	Set of gas-fired generating units.
GP	Set of node pair (m, n) for pipeline from node m to node n.

$\mathrm{GC}\,(m)$	Set of nodes connected with m.
α, β, γ	Fuel function coefficient of natural gas-fired unit.
$F^{\max}$	Contracted amount for natural gas-fired unit.
$\omega^{\min}, \omega^{\max}$	Minimum and maximum pressure.
$\nu^{\min}, \nu^{\max}$	Minimum and maximum of gas injection.
A	Node-gas supplier incidence matrix.
B	Node-gas load incidence matrix.
C	Bus-generator incidence matrix.
D	Bus-electrical load incidence matrix.
E	Bus-branch incidence matrix.

I. Introduction

NATURAL gas and renewable energy are the two most vital energy resources in the electric power industry's transition to an environmental-friendly operation. The use of natural gas and renewable energy in electric power sector has grown significantly in recent years. The U.S. natural gas consumption by the electric power sector increased from 34% of the total consumption in 2011 to 39% in 2012 [1]. Meanwhile, the natural gas-fired units accounted for 40% of the total existing generating capacity in 2012. The attractive utilization of shale gas has introduced the lowest natural gas prices in a decade, which may further expand the investments on natural gas-generating plants in electric power systems. Natural gas-fired units are expected to serve more than 50% of the peak electricity demand in the North America by 2015.

On the other hand, renewable energy has long held the promise of making significant contributions to the future of electric power systems. In addition, technological advancements in distributed control, off-grid generation and microgrid applications, and various government incentives have demonstrated a rapid growth in renewable energy deployments and utilizations throughout the world. The renewable energy accounted for about 5% of the total installed capacity by 2011, which mainly included wind, geothermal, biomass, and solar [2]. The installed wind capacity in the United States grew five times between 2005 and 2012 to approximately 50 GW. However, wind energy (including offshore) remains to be a critical part of electricity supply over the next decades [3].

Natural gas and renewable energy operations appear to be complementary in many respects concerning fossil fuel price and availability, environmental impacts, variability of renewable resources, and accessibility of such resources in load centers. Hence, the coordination between natural gas and renewable energy in integrated resource planning would need to be reinforced.

1) Natural gas has experienced significant price variations, which would directly affect the cost of commitment and generation of generating units [4]. Also, a growing level of natural gas consumption by the electric power sector has increase challenges associated with natural gas transmission network planning and operation. A pressure loss or interruption in natural gas pipelines could lead to the loss of multiple natural gas-fired generators and raise the power system security concerns. On the contrary, variable renewable energy units have zero fuel costs and relatively fixed operating cost when adequately distributed throughout a geographic region [5].
2) Additional environmental emission regulations are being proposed to promote the further use of clean energy in the near future [6]. Renewable energy will not be subject to certain environmental constraints which offer additional benefits to long-term electric power system operations. Accordingly, the proliferation of natural gas-fired and renewable energy units in electric power systems could be heightened as more stringent low-carbon thresholds are enforced globally.
3) While the renewable generation does not incur fuel costs or emission caps, it experiences resource variability and low-capacity factor values. These uncertain characteristics of renewable energy introduce new challenges and additional costs to the power system operations [7]. The variability of large-scale wind energy may have intense impacts on power system operations. The natural gas units can offer flexible dispatch and quick ramping capability in such cases for firming power system operations.

The interdependency of electricity and natural gas is addressed in [8]–[11]. The natural gas flow network is modeled in [8] by daily and hourly limits on pipelines, subareas, plants, and generating units for assessing the power system security. An approach for solving the seasonal operation planning problem of a hydrothermal system was discussed in [9] where part of the thermal capacity consists of energy-constrained natural gas flow. The short-term scheduling of integrated natural gas transmission and hydrothermal power system was considered in [10] by applying Lagrangian relaxation and dynamic programming. The augmented Lagrangian relaxation method was adopted in [11] for solving the coordinated scheduling of interdependent hydrothermal power and natural gas systems.

The impact of uncertainties on power system operation caused by variable wind energy was discussed in [12] and [13]. A stochastic model of wind energy was proposed in [12] for the optimal operation of energy storage units in which hybrid genetic algorithm and neural network methods were employed to solve the uncertain problem. A stochastic optimal scheduling model for treating hourly wind energy and load forecasts as variables was considered in [13] for studying the impact of high wind energy penetrations on the Irish power system operation. Other system uncertainties including components outages, load forecast errors, and water inflow are considered in [14] for a midterm stochastic security constrained unit commitment model to optimize water and natural gas supplies.

The main contribution of this paper is to discuss the coordination between the electricity and the natural gas infrastructures based on an integrated stochastic model (referred to as EGTran) for firming the variability of wind energy. EGTran considers natural gas transmission constraints and the variability of wind energy in the optimal short-term operation of stochastic power systems. The scenario-based approach considers the autoregressive moving average (ARMA) time series for representing wind energy variations. This integrated EGTran model minimizes the total expected operation cost of all scenarios while satisfying electric power system security and network constraints. The scenario reduction is adopted in EGTran as a

tradeoff between the calculation speed and the solution accuracy. A decomposition approach is applied so that the natural gas allocation problem considering nonlinear natural gas transmission constraints can be solved by the Newton–Raphson substitution method. The system operators can use the proposed EGTran model for the short-term scheduling of energy assets with a high penetration of renewable energy in which the pipeline-constrained natural gas units offer the required ramping flexibility.

The rest of this paper is organized as follows. The integrated stochastic formulation is presented in Section II. Section III presents the solution methodology to handle the nonlinear natural gas network constraints. Section IV presents the case studies in a 6-bus system and the IEEE 118-bus system. The conclusion drawn from the study is provided in Section V.

II. EGTran Formulation

The EGTran formulation procures the wind energy forecast by incorporating the power curve of wind turbine and wind speed time series at wind energy sites. The wind speed forecast follows the Weibull distribution function using the Weibull constant and the average wind speed. The ARMA time-series model is applied to simulate wind speed variations [15]. Specifically, the wind speed forecast errors are represented by a time series in which the present observations are decreasingly dependent on past observations as traverse back in time. A lower order ARMA (1,1) time series is defined for simulating wind speeds as

$$X(t) = \alpha X(t-1) + Z(t) + \beta Z(t-1)$$

where $X(t)$ is the wind speed forecast error in t-hour forecast, α and β are constant parameters, and $Z(t)$ is the random Gaussian variable with mean equal to zero and standard deviation σ_z. A unique set of the three parameters α, β, σ_z describes an ARMA(1,1) time series. The real hourly wind speed $V(t)$ is calculated as the sum of the wind speed forecast and the wind speed forecast error, i.e.,

$$V(t) = V_f(t) + X(t).$$

We assume that historical wind data are available at each wind site. The standard deviation is represented by the truncated Gaussian distribution function $[-\sigma, +\sigma]$ in which the range of σ increases linearly in the forecast horizon.

The hourly wind speed is converted to energy by a typical power output curve of wind turbine as shown in Fig. 1. No power is generated at wind speeds below cut-in speed V_C; at wind speeds between rated wind speed V_R and cut-out wind speed V_F, the output is equal to the rated power of the generator; above cut-out wind speed, the turbine is shutdown.

Using the ARMA (1,1) time-series model, we create multiple scenarios (say u) to derive the boundary level by the maximum deviations in wind speed scenarios from forecasted values. The corresponding scenario tree has u scenarios and each scenario can be considered as a path with a possibility of $1/u$. The computational requirement for solving scenario-based scheduling problems ascends rapidly with the number of

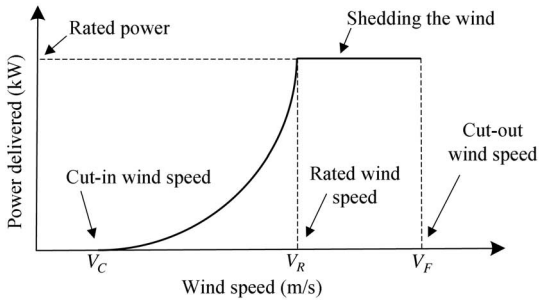

Fig. 1. Typical power curve of wind turbine.

scenarios. Therefore, a scenario reduction method is adopted as a tradeoff between the computation efficiency and the modeling accuracy [16]. The scenario reduction technique is a scenario-based approximation with a smaller number of scenarios representing a reasonably approximation of the original system by measuring a distance of probability distributions as a probability metric. After the scenario reduction, each scenario represents a possible wind energy profile, in which $\Pr_s$ is assigned as weight to reflect the possibility of occurrence of each scenario.

The proposed stochastic model of EGTran is used to determine the hourly security-constrained schedule for minimizing the expected cost of supplying the electrical load over the scheduling horizon while satisfying various system constraints. The objective function is defined as

$$\begin{aligned}\min \sum_{s=1}^{N_S} \Pr_s \Bigg\{ & \sum_{t=1}^{N_T} \sum_{i \in GU} \left(W_{i,t}^{s,\text{gas}} + \text{SU}_{i,t} + \text{SD}_{i,t} \right) \\ & + \sum_{t=1}^{N_T} \sum_{i \notin \text{GU}} \left(F_i^c(P_{i,t}^s) \cdot I_{i,t}^s + \text{SU}_{i,t} + \text{SD}_{i,t} \right) \\ & + \text{VOLL} \cdot \sum_{t=1}^{N_T} \sum_{b=1}^{N_B} \text{DL}_{b,t}^s \Bigg\}. \end{aligned} \quad (1)$$

The first term in the objective function (1) is the natural gas contract cost and startup/shutdown costs for natural gas-fired generating units. The second term is the generation cost of other units, which includes fuel and startup/shutdown costs. The third term is the estimated cost of load shedding. The load shedding price is the value of lost load (VOLL), which is expressed in \$/kW/h.

A. Power System and Unit Constraints

For each period t in scenario s, the power system and unit constraints are expressed as follows.

System load balance constraints

$$\sum_{i=1}^{N_U} P_{i,t}^s \cdot I_{i,t}^s + \sum_{i=1}^{N_W} P_{w,t}^s = \sum_{b=1}^{N_B} (\text{DE}_{b,t} - \text{DL}_{b,t}^s) \quad \forall t, \forall s. \quad (2)$$

System spinning reserve constraints

$$\sum_{i=1}^{N_U} \text{SR}_{i,t}^s \cdot I_{i,t}^s \geq R_t \quad \forall t, \forall s. \quad (3)$$

Generating unit constraints: The physical constraints of generating units include unit capacity limits (4), ramp rate limits (5), and minimum ON/OFF time (6)

$$P_i^{\min} I_{i,t}^s \le P_{i,t}^s \le P_i^{\max} I_{i,t}^s \qquad \forall t, \forall s \tag{4}$$

$$\begin{aligned} P_{i,t}^s - P_{i,(t-1)}^s &\le [1 - I_{i,t}^s (1 - I_{i,(t-1)}^s)] R_i^{up} \\ &\quad + I_{i,t}^s (1 - I_{i,(t-1)}^s) P_i^{\min} \qquad \forall t, \forall s \\ P_{i,(t-1)}^s - P_{i,t}^s &\le [1 - I_{i,(t-1)}^s (1 - I_{i,t}^s)] R_i^{dn} \\ &\quad + I_{i,(t-1)}^s (1 - I_{i,t}^s) P_i^{\min} \qquad \forall t, \forall s \end{aligned} \tag{5}$$

$$\begin{aligned} (X_{i,(t-1)}^{s,\text{on}} - T_i^{\text{on}})(I_{i,(t-1)}^s - I_{i,t}^s) \ge 0 \qquad \forall t, \forall s \\ (X_{i,(t-1)}^{s,\text{off}} - T_i^{\text{off}})(I_{i,t}^s - I_{i,(t-1)}^s) \ge 0 \qquad \forall t, \forall s. \end{aligned} \tag{6}$$

Load shedding constraints: Load shedding is considered in the EGTran objective to provide a feasible solution under extreme situations when the coordinated system cannot meet its load. The load shedding at each bus is limited to a predefined amount which is given as

$$\text{DL}_{b,t}^s \le \text{DL}_{b,t}^{\max} \quad \forall t, \forall s. \tag{7}$$

Power transmission flow constraints: Constraint (8) shows the power balance at each bus. Constraint (9) represents the power flow from bus j to bus k, which is limited by the transmission line capacity (10). Constraint (11) sets the voltage angle of the reference bus to zero

$$E \cdot \text{pf}^s = C \cdot P_{i,t}^s - D \cdot \left(\text{DE}_{b,t} - \text{DL}_{b,t}^s\right) \quad \forall t, \forall s \tag{8}$$

$$pf_{br}^s = (\theta_j^s - \theta_k^s)/x_{jk} (j,k \in br) \tag{9}$$

$$|pf_{br}^s| \le \text{pf}_{\text{br}}^{\max} \tag{10}$$

$$\theta_{\text{ref}} = 0. \tag{11}$$

Constraints (2) and (8) are used in master unit commitment problem and power transmission network feasibility subproblem, respectively. The master unit commitment problem would determine the unit commitment status and dispatch considering the system and load balance equation in constraint (2). Constraint (8) represents the power balance at each bus of the power system, which would be used in the subproblem to calculate and check the power flow along with constraints (9)–(11).

B. Wind Generation and System Emission Constraints

Wind generation constraints: The dispatched wind power generation for each period t in scenario s is limited by the hourly wind energy output, which is calculated based on the power curve and hourly wind speed

$$P_{w,t}^s \le \text{PW}_{w,t}^f \quad \forall t, \forall s. \tag{12}$$

System emission constraints: The operation of fossil-fueled thermal units (i.e., coal and oil) could be curtailed by emission constraints. Composed primarily of methane, the byproducts of natural gas combustion are carbon dioxide and water vapor. Therefore, natural gas-fired units often meet the existing SO_2 and NO_x emission constraints while still facing carbon emission constraints. In each scenario s, the regional/system carbon emission during the scheduling horizon for a group of generation units $i \in EG$ must not exceed the emission allowance represented by

$$\sum_{i \in \text{EG}} \sum_{t=1}^{N_T} [F_i^e(P_{i,t}^s) \cdot I_{i,t}^s + \text{SU}_{i,t}^e + \text{SD}_{i,t}^e] \le \text{EMS}^{\max} \quad \forall s \tag{13}$$

in which

$$F_i^e(P_{i,t}^s) = a_i^e + b_i^e P_{i,t}^s + c_i^e (P_{i,t}^s)^2 \quad \forall t, \forall s \tag{14}$$

and a^e, b^e, c^e are the coefficients of the carbon emission functions for unit i. The startup/shutdown emission levels are represented by SU^e, SD^e in $i \in \text{EG}$.

C. Coupling Constraints for Electricity and Natural Gas

1) Fuel Constraints for Gas-Fired Units: Natural gas-fired power plants would interface natural gas and electricity infrastructures. As the largest industrial consumer of natural gas, electric generators usually rely on interruptible gas transportation services to meet their fuel requirements. The interruptible service representing the lowest service priority is usually priced solely on a volumetric basis. For each period t in scenario s, the fuel cost for a natural gas-fired unit is determined by its natural gas consumption and the price of natural gas contract (15). The natural gas consumption $F_{i,t}^{s,\text{gas}}$ is determined by the hourly dispatch of natural gas-fired unit (16). Each natural gas supply contract is considered as load (obligation) for the natural gas network (17), which cannot exceed the natural gas day contract (18)

$$W_{i,t}^{s,\text{gas}} = (\rho_{\text{gas}}) F_{i,t}^{s,\text{gas}} \quad (i \in \text{GU}, \forall t, \forall s) \tag{15}$$

$$F_{i,t}^{s,\text{gas}} = \alpha + \beta P_{i,t}^s + \gamma (P_{i,t}^s)^2 \quad (i \in \text{GU}, \forall t, \forall s) \tag{16}$$

$$L_{l,t}^s = F_{i,t}^{s,\text{gas}} \quad (i \in \text{GU}, \forall t, \forall s) \tag{17}$$

$$\sum_{t=1}^{N_T} F_{i,t}^{s,\text{gas}} \le F_i^{\max} \quad (i \in \text{GU}, \forall s). \tag{18}$$

2) Natural Gas Transportation Constraints: Natural gas is transported from natural gas suppliers to end customers through an extensive natural gas transportation system [17]. The natural gas transportation system consists of a complex network of pipelines, storage, and compressors which transport the natural gas from wellheads or suppliers to local distribution companies or directly to large commercial and industrial users. The natural gas supply system usually consists of natural gas wells and storage facilities. The natural gas extracted from gas wells is processed at the gas processing plant near the wellhead and released to the natural gas transmission system. Similar to the electricity system, the natural gas system is composed of transmission (high-pressure) and distribution (low-pressure) pipelines. The transmission pipeline transports the processed natural gas from suppliers to regions with natural gas demands. The distribution pipelines operate at lower pressure levels,

which are adjusted by the associated pressure regulators for the local delivery of natural gas.

As one of the most complex nonlinear systems, the natural gas transmission system can be represented by its steady state and dynamic characteristics. The transient state of natural gas flow through a pipeline is described as a one-dimensional (1-D) dynamics along the axis of the natural gas pipeline, which requires distributed parameters and time-varying state variables [18]. The dynamic characteristics would introduce additional challenges in both the modeling and computation of our proposed problem. Therefore, we present a steady state natural gas flow model composed of a group of nonlinear equations in this work. From the mathematical viewpoint, the steady-state natural gas problem will determine the state variables including nodal pressures and flow rates in individual pipelines based on the known injection values of natural gas supply and load.

The natural gas flow between node m and n through a pipeline that does not utilize a compressor is stated as a quadratic function of the pressures at the two end nodes

$$f_{mn} = \mathrm{sgn}(\omega_m, \omega_n) \cdot C_{mn} \sqrt{|\omega_m^2 - \omega_n^2|} \tag{19}$$

$$\mathrm{sgn}(\omega_m, \omega_n) = \begin{cases} 1, & \omega_m \geq \omega_n \\ -1, & \omega_m < \omega_n \end{cases} \tag{20}$$

where the constant C_{mn} depends on pipeline characteristics (temperature, length, diameter, friction) and natural gas compositions. The direction of natural gas flow is determined by the incremental pressure between the two nodes (20).

The natural gas flow through pipelines is driven by the pressure difference between the two adjacent nodes. So, compressors usually installed at 40- to 100-mile intervals along the pipeline would ensure that the natural gas flow through any one pipeline is maintained at the desired pressure level. The natural gas flow through a pipeline with compressors is stated as (21), in which the pressure at the incoming node is lower than that at the outgoing node. The introduction of compressors for increasing the transmission capacity along a pipeline would heighten the pressure difference between the two end nodes

$$f_{mn} \geq \mathrm{sgn}(\omega_m, \omega_n) \cdot C_{mn} \sqrt{|\omega_m^2 - \omega_n^2|}. \tag{21}$$

Similar to the power transmission lines in which bus voltages are limited, the desired pressure at each node is bounded by its lower and upper limits as

$$\omega^{\min} \leq \omega \leq \omega^{\max}. \tag{22}$$

The flow conservation (23) would preserve the nodal balance for the natural gas flow. Mathematically, the nodal balance equation is stated as

$$\sum_{\mathrm{sp}=1}^{\mathrm{NGS}} \mathrm{Av}_{\mathrm{sp}} - \sum_{l=1}^{\mathrm{NGL}} \mathrm{BL}_l - \sum_{n \in \mathrm{GC}(m)} f_{\mathrm{mn}} = 0. \tag{23}$$

Natural gas storage facilities in the natural gas transportation system would usually link transmission and distribution pipelines. Storage facilities would ensure adequate supplies of natural gas for seasonal demand shifts and unexpected demand surges. Both gas wells and storage facilities are modeled as positive injections at related nodes with lower and upper limits

$$v_{\mathrm{sp}}^{\min} \leq v_{\mathrm{sp}} \leq v_{\mathrm{sp}}^{\max}. \tag{24}$$

Natural gas end users are commonly classified as residential, commercial, and industrial. While some large industrial, commercial, and electric generation customers receive natural gas directly from high-capacity interstate and intrastate transmission pipelines, most other users receive natural gas from a local distribution company. Natural gas consumption at any nodes is considered as a gas load, which is stated as

$$L_l^{\min} \leq L_l \leq L_l^{\max}. \tag{25}$$

D. Stochastic Optimal Solution Methodology for EGTran

Equations (1)–(25) represent a multistage stochastic optimization problem integrating the variable renewable energy with the natural gas network model. The unit commitment solution represents decision variables corresponding to time periods $1, \ldots, N_T$. In the multistage setting, the quantity of random wind energy is known in the respective time period. The scenarios that have the same history would not be distinguished, once we introduce nonanticipativity constraints, which unifies the decision variables $I_{i,t}^s$ in different scenario s within the same period t.

In order to handle the nonlinear constraints of natural gas pipeline flow, Benders decomposition [19] is applied to unbundle the proposed problem into a master problem (stochastic unit commitment) and natural gas network subproblem as shown in Fig. 2. Here, the input data corresponding to the hourly wind speed forecast and wind turbine output curve are used to generate wind energy scenarios in which ARMA(1,1) time series is applied to simulate wind speed variations. Fewer scenarios are then identified by the scenario reduction method in which each scenario represents a possible state of wind energy output. Then, a stochastic master unit commitment problem will be solved without considering electric power transmission network constraints (8)–(11) and coupling constraints representing electricity and natural gas systems (15)–(25).

Using the commitment solution, the power transmission network subproblem will check the electric power flow based on the unit dispatch. If any power flow violations are found, the feasibility cuts will be added to the previous master problem for recalculating the new commitment solution. Here, the feasibility cuts is generated from a dc power flow model [constraints (8)–(11)], which will eliminate the overloaded lines by enforcing limits on corresponding generating unit output. After the power transmission feasibility check, the hourly natural gas consumption is determined by the hourly dispatch of natural gas-fired units. Then, the natural gas network subproblem will check the availability of natural gas resource and whether it can satisfy natural gas transmission limits and the gas demand required by the natural gas-fired units that are committed by the unit commitment problem in each scenario.

Natural gas usage cuts are generated from the solution of a natural gas allocation problem with nonlinear equations, which

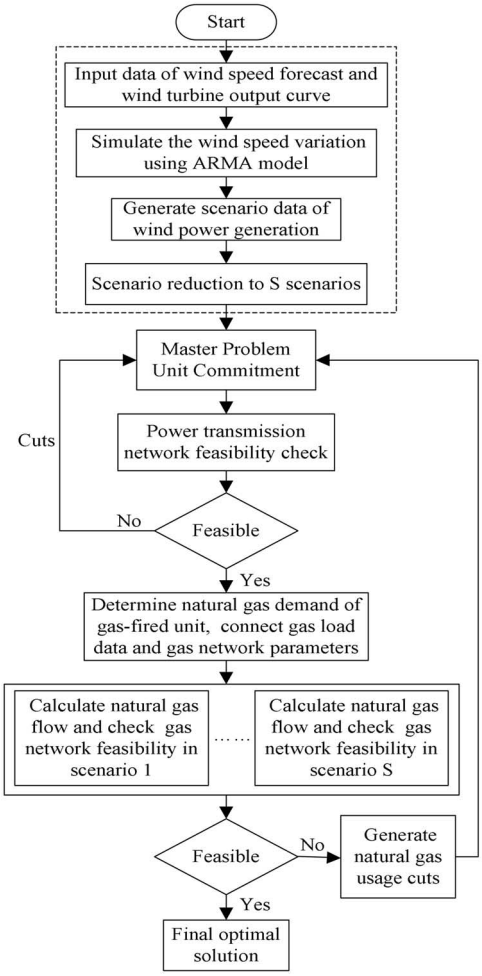

Fig. 2. Stochastic infrastructure coordination model of EGTran.

is solved by Newton–Raphson substitution method [20]. In the natural gas network feasibility subproblem, we will add a nonnegative natural gas load-shedding variable at each delivery point, which represents the virtual load shedding of natural gas, to ensure that the gas allocation problem is feasible. If the cumulative amount of load shedding is larger than the specified tolerance, which means that the solution is infeasible, the corresponding cuts for natural gas usage violation will be generated and fed back to the unit commitment problem for the next iteration. The cuts representing the shortages of natural gas supply will limit the gas consumption ($F_{i,t}^{s,\text{gas}}$) by certain natural gas-fired units and resort to other options for supplying the electrical load. This iterative process will be repeated until we get the final optimal solution when all violations are eliminated.

III. Numerical Simulations of EGTran

We use two case studies consisting of a 6-bus power system with a 6-node natural gas system and the IEEE 118-bus system with a 10-node natural gas system to demonstrate the effectiveness of the stochastic EGTran model. The pipeline-constrained natural gas units are utilized in EGTran to firm the variability of wind energy as grid operators minimize the day-ahead operating cost.

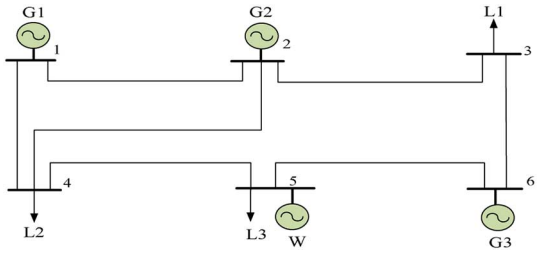

Fig. 3. Six-bus power system.

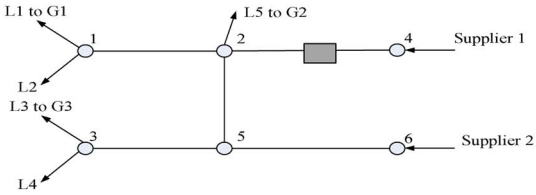

Fig. 4. Six-node natural gas system.

A. Six-Bus System

The six-bus system, depicted in Fig. 3, has three gas-fired units (G1, G2, G3) and one wind farm (W), seven transmission lines, and three loads. The six-node natural gas system is given in Fig. 4, which has five pipelines, one compressor, two natural gas suppliers, and five natural gas loads. Natural gas loads 1, 3, 5 represent the hourly generation dispatch of three gas-fired units. Natural gas loads 2 and 4 represent other types of natural gas end users. $\text{DL}_b^{\max}$ is assumed to be 20% of the load forecast at each bus as we assume that the demand cannot be completely curtailed for the sake of the customers. The electrical and natural gas system data are given in motor.ece.iit.edu/data/Gastranssmion6_2.xlsx.

We consider the following cases.

Case 1: The impact of gas price volatility and fuel availability on natural gas-constrained system (with/without a fixed 20-MW wind energy).

Case 2: Effect of emission constraints on the EGTran solution (with/without a 20-MW wind energy system) is considered.

Case 3: Variable wind energy is considered in a deterministic case (i.e., wind forecast errors are not considered).

Case 4: The stochastic EGTran solution with variable wind energy and wind forecast errors is considered.

These cases are discussed as follows.

Case 1: In order to analyze the effect of zero fuel cost wind energy operation on the EGTran solution, we take into account two cases with/without a fixed 20-MW wind energy system. The capacity of G1 is decreased to 200 MW, when 20 MW wind energy is considered, in order to retain the same total system capacity of 320 MW. Wind energy forecast errors are not taken into account in this case. In Table I, the cheapest unit G1 is always committed. The expensive unit G2 is committed between hours 10 and 22 and Unit G3 is committed between hours 8 and 24 when the wind unit is not utilized. The daily operation cost is \$97 104. However, when the fixed 20-MW wind energy system is introduced, the expensive units G2 and

TABLE I
HOURLY SCUC IN CASE 1: 6-BUS SYSTEM

Daily production cost: $97 104 (without wind energy)																								
Unit	Hours (0–24)																							
G1	1	1	1	1	1	1	1	1	1	1	1	1	1	1	1	1	1	1	1	1	1	1	1	1
G2	0	0	0	0	0	0	0	0	0	0	1	1	1	1	1	1	1	1	1	1	1	1	0	0
G3	0	0	0	0	0	0	0	0	1	1	1	1	1	1	1	1	1	1	1	1	1	1	1	1
Daily production cost: $87 190 (with 20 MW wind energy)																								
Unit	Hours (0–24)																							
G1	1	1	1	1	1	1	1	1	1	1	1	1	1	1	1	1	1	1	1	1	1	1	1	1
G2	0	0	0	0	0	0	0	0	0	0	0	1	1	1	1	1	1	1	1	1	1	1	0	0
G3	0	0	0	0	0	0	0	0	0	1	1	1	1	1	1	1	1	1	1	1	1	1	0	0
W	1	1	1	1	1	1	1	1	1	1	1	1	1	1	1	1	1	1	1	1	1	1	1	1

TABLE II
COMPARISON OF RESULTS IN CASE 1

Scenario	Natural gas price up by 20%		Natural gas load L4 is increased by 500 kcf/h	
	Without wind unit	With 20 MW wind	Without wind unit	With 20 MW wind
Daily production cost ($)	111 197	98 710	95 841	87 059
Load shedding cost ($)	0	0	35 080	3 480
Total cost ($)	111 197	98 710	130 921	90 539
Load shedding (MW)	0	0	35.08	3.48

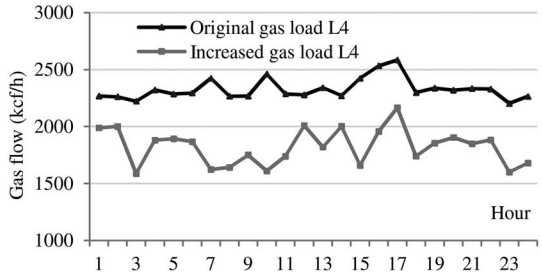

Fig. 5. Comparison of gas flow from pipeline node 2 to node 5.

G3 are committed less and the operation cost is decreased to $87 190 because wind energy does not incur any fuel costs.

In Case 1, we also analyze two EGTran scenarios for the natural gas price volatility and the natural gas availability.

Scenario 1: Increase the natural gas price for unit G1 by 20%.

In Table II, the daily operation cost without wind energy is $111 197 in Scenario 1, which is lowered to $98 710 when we add 20 MW of wind energy. The operation cost of Scenario 1 is higher than that of the base case (in Table I) because the gas price for G1 is increased and G1 is the largest unit with 68% of the total system capacity. The system operation cost is directly affected by the volatility of natural gas prices.

Scenario 2: Increase the residential natural gas load L4 by 500 kcf/h (i.e., reduce the natural gas availability to plants).

In Scenario 2, the residential natural gas load L4 is increased by 500 kcf/h, which could represent severe weather conditions. In the 6-node natural gas system, pipeline extending from node 5 to node 2 plays a critical role in interconnecting the two natural gas suppliers. As shown in Fig. 5, the natural gas flow through this pipeline that supplies G2 would be reduced

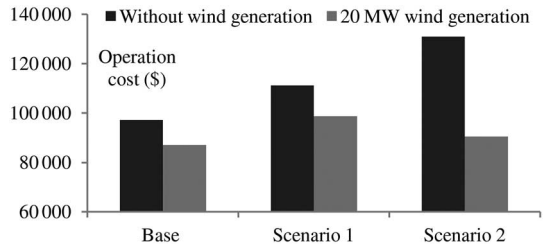

Fig. 6. Comparison of daily operation costs.

TABLE III
EMISSION EQUIVALENT CURVE OF UNITS

Unit	af (lb/MW^2/h)	bf (lb/MW/h)	cf (lb)
G1	0.0009	2.7	353.9
G2	0.0001	8.6	129.9
G3	0.01	35.3	274.8

TABLE IV
HOURLY SCHEDULE OF CASE 1 OF SIX-BUS SYSTEM

Daily production cost: $126 426 (with emission constraints)																								
Unit	Hours (0–24)																							
G1	1	1	1	1	1	1	1	1	1	1	1	1	1	1	1	1	1	1	1	1	1	1	1	1
G2	1	1	1	1	1	1	1	1	1	1	1	1	1	1	1	1	1	1	1	1	1	1	1	1
G3	0	0	0	0	0	0	0	0	0	0	0	0	0	0	0	0	1	0	0	0	0	0	0	0

because the residential gas load L4 has a higher priority. This fuel shortage for operating G2 would further result in a 35-MW curtailment of electricity load at bus 4 between hours 15 and 19, which would increase the daily operation cost to $130 921. However, as wind energy is introduced at bus 5, the proposed load shedding is reduced to 3.48 MW because wind energy can supply loads at bus 4. This alleviation of supply shortage would effectively lower the daily operation cost to $90 539 as demonstrated in Fig. 6.

This case also demonstrates that the fuel availability would greatly affect the operation cost of a natural gas-constrained power system. However, wind energy does not experience the same market-based fuel supply concerns and price volatility as that of natural gas-fired generation. Therefore, the integration of wind energy can play a complementary role in hedging the risk of fuel-constrained generation uncertainty.

Case 2: The carbon dioxide emission coefficients of the three natural gas units are shown in Table III. The system emission threshold is set at $10.8{*}10^5$ lbs.

Without wind energy: Without emission constraints, the expensive unit G2 is committed between hours 10 and 22 and the daily operation cost is $97 104 as shown in Case1. When emission constraints are considered, Table IV shows that unit G2 is committed continuously since G1 is more pollutant. The daily operation cost is increased to $126 426 when emission constraints are considered.

With wind energy: The installed wind energy capacity at bus 5 is 20 MW, which represents 6.25% of the total system capacity. The capacity of G1 is decreased to 200 MW to retain the total generation capacity at 320 MW. The utilization of wind energy in this case would reduce the system operation cost to $106 744 by alleviating emission constraints. Fig. 7 shows that

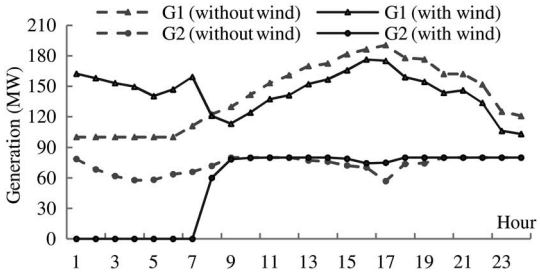

Fig. 7. Hourly dispatch of units G1 and G2.

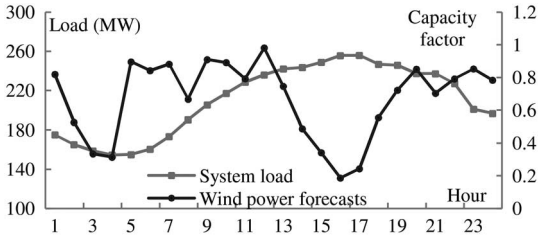

Fig. 8. Load profile and wind energy forecasts.

TABLE V
HOURLY DISPATCHED WIND ENERGY

HR	Wind power (MW)	Load shedding (MW)	HR	Wind power (MW)	Load shedding (MW)	HR	Wind power (MW)	Load shedding (MW)
1	78.69	0	9	87.37	0	17	23.41	13.71
2	50.56	0	10	85.61	0	18	53.26	0
3	32.12	0	11	76.11	0	19	69.35	0
4	30.18	0	12	94.26	0	20	81.72	0
5	58.16	0	13	71.68	0	21	67.56	0
6	63.69	0	14	46.87	0	22	76.04	0
7	76.86	0	15	32.81	0	23	81.86	0
8	64.04	0	16	17.93	18.97	24	75.27	0

the cheaper and pollutant unit G1 is dispatched more, whereas the expensive unit G2 is dispatched less. This is because zero-emission wind generation free up emission load for cheaper unit G1 that can be scheduled additionally considering the same emission threshold. From the long-term perspective, the wind energy integration is not subject to environmental compliance criteria, which could bring additional revenue should the emission regulation become increasingly stringent.

Case 3: In this case, the available wind energy is 96 MW, which represents 30% of the system capacity. The hourly capacity factor is the ratio of the wind energy forecast to the wind energy capacity. Fig. 8 shows the available load and wind energy forecast. In Table V, load shedding occurs when the wind energy is below 20 MW at peak hours 16 and 17. G1, G2, and G3 are dispatched at 124 MW, 80 MW, and 20 MW, respectively, at hour 16 with an additional load shedding for compensating the lower availability of wind energy.

The ramping capability of thermal units would accommodate the wind energy variability for maximizing the utilization of wind generation. The base ramping rates for the three thermal units are 55 MW/h, 40 MW/h, and 5 MW/h, respectively. For comparison, we increase the ramping rates to 120 MW/h, 80 MW/h, and 20 MW/h, respectively. Fig. 9 shows that higher rates of thermal ramping would accommodate a higher level of

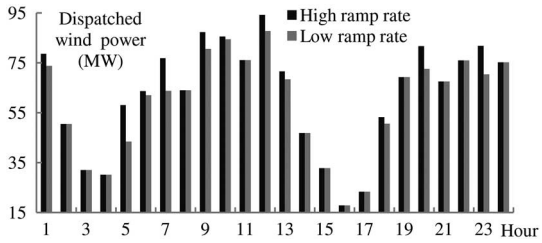

Fig. 9. Hourly dispatched of wind energy unit.

wind energy. The ramping rate of G1 is crucial as this thermal unit is committed more often.

In Table VI, we vary the wind energy penetration level from 5% to 30%. However, the total system capacity will remain the same by lowering the G1 capacity. In Table VI, the daily operation cost decreases when the wind energy penetration is smaller than 15%. This is because the wind energy would accommodate the power system with a quick ramping of thermal units and without incurring any fuel costs. However, load shedding would occur at a higher daily production cost when the wind energy penetration reaches 20%. This is mainly caused by a lower availability of wind energy at hour 16 and 17 when the quick-ramping capability is insufficient for picking up the load supplied by wind energy. While the variable wind energy does not incur any fuel costs, it does experience dynamic resource variability in an hourly or shorter time scales. This example supports the notion that a balanced electricity portfolio with conventional power (e.g., natural gas) and renewable energy can result in a steady optimization of generation resource availability, fuel cost, and environment requirement.

Case 4: In this case, the wind speed forecast follows a Weibull distribution function with a Weibull constant of 2 and the average wind speed of 6.5 m/s. The first-order ARMA (1,1) time series is created to simulate wind speed forecast errors. The Wind energy curve is procured based on the wind speed and wind turbine power output curve. Fig. 10 shows that the wind energy forecast error increases gradually with the forecasting time period. Here, the instantaneous wind energy forecast error at times is enlarged compared to the wind speed forecast error, which is due to the nonlinear characteristics of wind turbine power curve as shown in Fig. 1. We generate 3000 scenarios and 10 are retained after scenario reduction.

The expected operation cost for the 10 scenario solution is $88 952 and the forecast wind energy in the 24-h scheduling horizon is 306 MW/h. The operation cost deviation in each scenario is mainly caused by the amount of utilized wind energy since it does not incur any fuel cost. As shown in Table VII, Scenarios 2, 4, 6, 7, and 9 utilize more wind energy, thus requiring less generation supplied by conventional natural gas-fired units and lower operation cost.

B. IEEE 118-Bus System

The modified IEEE 118-bus system has 76 thermal generators including 54 fossil units, 12 gas-fired units, 7 wind farms, 186 branches, and 91 load buses. The total capacity of natural gas-fired units and wind energy are 1075 MW and 720 MW, respectively, which account for 11% and 8%

TABLE VI
RESULTS FOR WIND PENETRATION LEVELS

Wind penetration (%)	5%	10%	15%	20%	25%	30%
Wind unit cap. (MW)	16	32	48	64	80	96
Daily product. cost ($)	92 104	85 120	80 722	78 232	75 896	73 497
Load shedding (MW)	0	0	0	4.15	15.95	32.68
Load shedding cost ($)	0	0	0	4150	15950	32680
Total cost	92 104	85 120	80 722	91 847	106 177	115 516

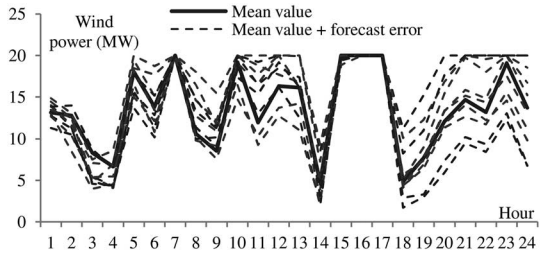

Fig. 10. Wind energy forecast.

TABLE VII
COMPARISON OF RESULTS FOR DIFFERENT SCENARIO

Scenario	S1	S2	S3	S4	S5
Probability	0.0772	0.0832	0.1271	0.0786	0.1192
Wind power (MW/h)	286.08	359.14	273.94	318.13	277.24
Production cost ($)	89482.7	87697.1	89780.8	88621.0	89593.3
Scenario	S6	S7	S8	S9	S10
Probability	0.1025	0.1396	0.0908	0.0960	0.0858
Wind power (MW/h)	344.55	344.56	268.85	311.46	276.62
Production cost ($)	88127.4	87988.6	89923.8	88769.5	89621.1

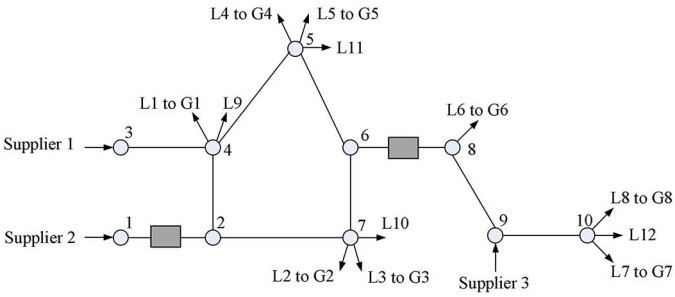

Fig. 11. Ten-node natural gas system.

of the total generation capacity. The natural gas network consists of ten nodes, ten pipelines, and two compressors as shown in Fig. 11. L1 through L8 are gas loads consumed by natural gas Units 1–8, respectively. L9 through L12 are fixed residential gas loads. DL_b^{max} is again assumed to be 20% of the load forecast at each bus. The 118-bus power system and 10-node gas system data are given in motor.ece.iit.edu/data/Gastranssmion_118_10_1.xls.

At first, we assume that the wind energy forecast error is zero and 10 862 MW/h of wind energy is utilized. The deterministic daily production cost is $1 918 361, which indicates that the natural gas units cannot be fully committed because of the gas shortage in the scheduling horizon. Next we consider the stochastic nature of the system, while the system scale and the number of scenarios will dramatically increase the computation burden. Thus, the original 3000 scenarios are reduced to 5 with a computation time that is 235 s for executing the five scenarios in 118-bus system.

TABLE VIII
RESULTS FOR SCENARIOS

Scenario	S1	S2	S3	S4	S5
Probability	0.171	0.124	0.356	0.206	0.143
Wind Energy (MW/h)	11 278	10 415	11 485	11 899	10 503
Production cost ($)	1 840 592	1 984 198	1 808 369	1 748 574	1 977 425

When the wind energy forecast errors based on first-order ARMA (1,1) time-series model are introduced, the expected operation cost for the 5th scenario solution is $1 847 539. As shown in Table VIII, scenarios 1, 3, and 4 would adopt more wind energy and correspondingly bring out lower scenario system operation costs. Meanwhile, thermal units can provide the necessary ramping capability to integrate the variable wind generation, which makes larger power system demonstrate more robustness than the six-bus system.

IV. DISCUSSIONS

Based on the numerical results offered by case studies, we list our observations as follows.

1) EGTran provides the optimal hourly schedule for pipeline constrained natural gas units in electric power systems with variable wind energy units.
2) The constrained natural gas availability and the natural gas prices volatility would greatly affect the hourly thermal unit commitment and the power system operation cost. The wind energy with zero fuel cost can play a complementary role in hedging the risk from fuel availability and price volatility for conventional gas-fired generation.
3) The environmentally sustainable wind energy can help alleviate emission constraints, which may result in a lower cost considering the same emission threshold.
4) The flexibility and quick ramping capability of natural gas-fired units make them ideal electricity resource for firming the variability of wind energy.

In this work, we aim at discussing the coordination between the electricity and the natural gas infrastructures for firming the variability of wind energy. Therefore, in the proposed integrated stochastic model, we only consider systems uncertainties from the unpredictable wind energy in this step, while we

assume that the system operates in a normal state. The contingency analysis can easily be incorporated into this model by introducing contingency constraints associated with the system infrastructures [21].

V. Conclusion

In this paper, a short-term stochastic model is proposed to study the coordination of constrained natural gas and wind energy units in power systems. The proposed EGTran model integrates the natural gas network constraints, emission limits, and wind energy variability. The MIP approach is used to solve the integrated model. The Benders decomposition is adopted to separate the natural gas network feasibility check problem from the master power system problem, whereas the natural gas allocation problem is solved by the Newton–Raphson substitution method. The numerical results show that the wind energy could help reduce the power system dependence on the constrained natural gas network. The wind energy is not subject to the risk pertaining to the fuel availability, price volatility, or low environmental emission measures, which can also lower the operation cost and satisfy low-carbon compliance policies. On the other hand, higher penetration of wind energy may lead to the dispatch of more expensive units or even load shedding, if a sufficient level of quick-ramping thermal units is unattainable, to pick up the load when the wind speed drops rather quickly. As shown in this paper, the higher flexibility of natural gas-fired units would complement the additional integration of variable wind energy in electric power systems.

Acknowledgment

The authors acknowledge and appreciate the technical and financial support provided by Deanship of Scientific Research at King Abdulaziz University in Jeddah, Saudi Arabia.

References

[1] EIA. (2011). *Annual Energy Review* [Online]. Available: http://www.eia.doe.gov/emeu/aer/

[2] NREL. (2011) [Online]. Available: http://www.nrel.gov/

[3] National Renewable Energy Laboratory, "20% wind energy by 2030: Increasing wind energy's contribution to U.S. electricity supply," Tech. Rep. DOE/GO-102008-2567, 2008 [Online]. Available: http://www.20percentwind.org/

[4] M. Bolinger, R. Wiser, and W. Golove, "Accounting for fuel price risk when comparing renewable to gas-fired generation: The role of forward natural gas prices," Lawrence Berkeley Nat. Lab., Berkeley, CA, USA, Tech. Rep. LBNL-54751, 2004.

[5] N. Keyaerts, Y. Rombauts, E. Delarue, and W. D'haeseleer, "Impact of wind power on natural gas market: Inter market flexibility," in *Proc. 7th Int. Conf. Eur. Energy Market*, 2010, pp. 1–6.

[6] A. Lee, O. Zinaman, and J. Logan, "Opportunities for synergy between natural gas and renewable energy in the electric power and transportation sectors," Nat. Renew. Energy Lab., Golden, CO, USA, Tech. Rep. NREL/TP-6A50-56324, 2012.

[7] B. Bush, T. Jenkin, D. Lipowicz, and D. J. Arent, "Variance analysis of wind and natural gas generation under different market structures: Some observations," Nat. Renew. Energy Lab., Golden, CO, USA, Tech. Rep. NREL/TP-6A20-52790, 2012.

[8] T. Li, M. Eremia, and M. Shahidehpour, "Interdependency of natural gas network and power system security," *IEEE Trans. Power Syst.*, vol. 23, no. 4, pp. 1817–1824, Nov. 2008.

[9] G. Skugge, J. A. Bubenko, and D. Sjelvgren, "Optimal seasonal scheduling of natural gas units in hydro-thermal power system," *IEEE Trans. Power Syst.*, vol. 9, no. 2, pp. 848–854, May 1994.

[10] C. Unsihuay, J. W. Marangon Lima, and A. C. Zambroni de Souza, "Short-term operation planning of integrated hydrothermal and natural gas systems," in *Proc. IEEE/PES Power Tech Conf.*, 2007, pp. 1410–1416.

[11] C. Liu, M. Shahidehpour, and J. Wang, "Application of augmented Lagrangian relaxation to coordinated scheduling of interdependent hydrothermal power and natural gas system," *IET. Gener. Transm. Distrib.*, vol. 4, no. 12, pp. 1314–1325, Dec. 2010.

[12] Y. Yuan, Q. Li, and W. Wang, "Optimal operation strategy of energy storage unit in wind power integration based on stochastic programming," *IET. Renew. Power Gener.*, vol. 5, no. 2, pp. 194–201, Mar. 2011.

[13] P. Meibom, R. Bath, B. Hasche, H. Brand, and C. Weber, "Stochastic optimization model to study the operational impacts of high wind penetrations in Ireland," *IEEE Trans. Power Syst.*, vol. 26, no. 3, pp. 1367–1379, Aug. 2011.

[14] L. Wu and M. Shahidehpour, "Optimal coordination of stochastic hydro and natural gas supplies in midterm operation of power systems," *IET. Gener. Transm. Distrib.*, vol. 5, no. 5, pp. 577–587, May 2011.

[15] L. Soder, "Simulation of wind speed forecast errors for operation planning of multi-area power systems," in *Proc. Int. Conf. Probab. Methods Appl. Power Syst.*, 2004, pp. 723–728.

[16] L. Wu, M. Shahidehpour, and Z. Li, "Comparison of scenario-based and interval optimization approaches to stochastic SCUC," *IEEE Trans. Power Syst.*, vol. 27, no. 2, pp. 913–921, May 2012.

[17] M. Shahidehpour, Y. Fu, and T. Wiedman, "Impact of natural gas infrastructure on electric power systems," *Proc. IEEE*, vol. 93, no. 5, pp. 1042–1056, May 2005.

[18] C. Liu, M. Shahidehpour, and J. Wang, "Coordinated scheduling of electricity and natural gas infrastructures with a transient model for natural gas flow," *Chaos*, vol. 21, no. 2, pp. 025102-1–025102-12, May 2011.

[19] A. M. Geoffrion, "Generalized Benders decomposition," *J. Optim. Theory Appl.*, vol. 10, no. 4, pp. 237–261, 1972.

[20] C. Liu, M. Shahidehpour, Y. Fu, and Z. Li, "Security-constrained unit commitment with natural gas transmission constraints," *IEEE Trans. Power Syst.*, vol. 24, no. 3, pp. 1523–1536, Aug. 2009.

[21] Y. Fu, M. Shahidehpour, and Z. Li, "AC contingency dispatch based on security-constrained unit commitment," *IEEE Trans. Power Syst.*, vol. 21, no. 2, pp. 897–908, May 2006.

Ahmed Alabdulwahab received the Ph.D. degree in electrical engineering from the University of Saskatchewan, Saskatoon, Canada, in 2003.

He is an Associate Professor with the Renewable Energy Research Group, Department of Electrical and Computer Engineering, King Abdulaziz University, Jeddah, Saudi Arabia. He has been a Consultant to the Electricity and Co-Generation Regulatory Authority in Saudi Arabia and a Visiting Scientist at Kinectrics and the University of Manchester, Manchester, U.K. His research interests include power system planning and reliability evaluations.

Abdullah Abusorrah received the Ph.D. degree in electrical engineering from the University of Nottingham, Nottingham, U.K., in 2007.

He is an Associate Professor with the Department of Electrical and Computer Engineering, King Abdulaziz University. He is the Coordinator of the Renewable Energy Research Group and Member of the Energy Center Foundation Committee, King Abdulaziz University. His research interests include power quality and system analyses.

Xiaping Zhang received the B.S. and M.S. degrees in electrical engineering from Shanghai Jiaotong University, Shanghai, China, in 2006 and 2009, respectively. Currently, she is pursuing the Ph.D. degree at Illinois Institute of Technology, Chicago, IL, USA.

Mohammad Shahidehpour (F'01) received the Ph.D. degree in electrical engineering from the University of Missouri, in 1981.

He is the Bodine Chair Professor and Director of Robert W. Galvin Center for Electricity Innovation at IIT. He is also a Research Professor with the Renewable Energy Research Group, King Abdulaziz University, Jeddah, Saudi Arabia.

Dr. Shahidehpour is the recipient of the Honorary Doctorate from the Polytechnic University of Bucharest, Bucharest, Romania, in 2009.